Noise-induced multistability in chemical systems: Discrete versus continuum modeling

Andrew Duncan,[1] Shuohao Liao,[1] Tomáš Vejchodský,[1,2] Radek Erban,[1,*] and Ramon Grima[3,†]

[1]*Mathematical Institute, University of Oxford, Radcliffe Observatory Quarter, Woodstock Road, Oxford, OX2 6GG, United Kingdom*

[2]*Institute of Mathematics, Czech Academy of Sciences, Žitná 25, CZ-115 67, Czech Republic*

[3]*School of Biological Sciences, Kings Buildings, Mayfield Road, University of Edinburgh, EH9 3JF, United Kingdom*

(Received 28 July 2014; published 10 April 2015)

The noisy dynamics of chemical systems is commonly studied using either the chemical master equation (CME) or the chemical Fokker-Planck equation (CFPE). The latter is a continuum approximation of the discrete CME approach. It has recently been shown that for a particular system, the CFPE captures noise-induced multistability predicted by the CME. This phenomenon involves the CME's marginal probability distribution changing from unimodal to multimodal as the system size decreases below a critical value. We here show that the CFPE does not always capture noise-induced multistability. In particular we find simple chemical systems for which the CME predicts noise-induced multistability, whereas the CFPE predicts monostability for all system sizes.

DOI: 10.1103/PhysRevE.91.042111 PACS number(s): 05.40.−a, 02.50.Ey, 87.18.Tt

I. INTRODUCTION

The dynamics of chemical and biochemical circuits is noisy whenever the number of molecules of at least one chemical species is small. The analysis of such circuits typically proceeds either via the chemical master equation (CME) or the chemical Fokker-Planck equation (CFPE). The latter is obtained from a truncation of the Kramers-Moyal expansion of the CME up to second-order derivatives and is hence regarded as a continuous approximation or an asymptotic representation of the CME in the limit of large system size [1,2].

For systems composed of only unimolecular reactions, the CFPE's prediction for the mean and variance of the molecule numbers is well known to be the same as those of the CME; for systems in which at least one reaction is bimolecular, the CFPE's predictions for the first two moments are not exact, but it has recently been shown that the accuracy is high over a wide range of molecule numbers [3,4]. The CFPE's ability to reproduce noise-induced oscillations predicted by the CME has been studied by a number of authors (see, for example, Refs. [5,6]). The accuracy of the CFPE's prediction for the probability distribution is, in contrast, not as well studied. In particular a question of wide interest is whether the CFPE's marginal probability distribution has generally the same number of maxima (modes) as the CME's marginal probability distribution.

It is clear by the CFPE's derivation that for cases where the multimodality exists at large system sizes (the volume for chemical systems), the CFPE and CME predict the same number of modes of the marginal probability distribution. This is termed deterministic multistability since each peak in the marginal probability distribution is associated with a stable solution of the rate equations. It follows that, for these cases, the multimodality in the CFPE solution stems from the drift term rather than from the diffusion term of the CFPE. It is also known that the CFPE overestimates the transition rates between the deterministic stable states corresponding to each mode [7]; however, in the present paper we are only concerned with the ability of the CFPE to predict the correct number of maxima of the CME's probability distribution.

Besides deterministic multistability there is also a phenomenon referred to as stochastic multistability, noise-induced multimodality, or noise-induced multistability. This describes the case where the marginal probability distribution of the CME switches from a unimodal to a multimodal distribution as the system-size is decreased below a critical value. The existence of such a phenomenon has been long known [8], yet its practical relevance to biology and ecology has only started to be appreciated in the past decade [9–12]. Given that noise-induced multimodality occurs at intermediate or small system sizes, it is unclear whether such a phenomenon is captured by the CFPE since the derivation of the latter does implicitly assume large system sizes. Curiously, recently it has been shown that the CFPE can capture the onset of noise-induced bimodality [12] for a particular system of reactions which models a colony of foraging ants collecting food from two sources. The remaining question is whether the CFPE can generically capture this phenomenon. In this article we show, by means of examples, that this is not the case. In particular our findings clarify that there are two distinct types of noise-induced multimodality and that only one of these types is captured by the CFPE.

II. SIMPLE GENE REGULATORY MODELS

A. A gene regulatory system with no feedback

We start by considering the following simple model of transcription regulation without feedback [9]:

$$G \underset{k_{\text{off}}}{\overset{k_{\text{on}}}{\rightleftharpoons}} G^*, \quad G \xrightarrow{k_1} G + P, \quad G^* \xrightarrow{k_2} G^* + P, \quad P \xrightarrow{c} \emptyset. \tag{1}$$

A gene can be in one of two states G and G^*; switching between these two states is random and each state is associated with a different rate of protein (P) formation. Once formed, the protein can also decay. This model is a simplification of more realistic gene models where the mRNA is explicitly modeled [13]. We consider the case where there are N genes such that the total number of G and G^* equals N at all times; although genes typically exist in one or two copies per cell, plasmids are

*erban@maths.ox.ac.uk
†ramon.grima@ed.ac.uk

 ©2015 American Physical Society

nowadays commonly used to genetically engineer cells with a large number of copies of a given gene [14], and hence our model is of biochemical relevance.

Denoting by t the time and by $\tau = ct$ the dimensionless time, the CME for the reaction system Eq. (1) is given by

$$\begin{aligned}\partial_\tau \Pi(n,p,\tau) = {} & q_{\text{off}}\left(E_n^{-1}-1\right)(N-n)\Pi(n,p,\tau) \\ & + q_{\text{on}}\left(E_n^{+1}-1\right)n\Pi(n,p,\tau) \\ & + q_1 n\left(E_p^{-1}-1\right)\Pi(n,p,\tau) \\ & + q_2(N-n)\left(E_p^{-1}-1\right)\Pi(n,p,\tau) \\ & + \left(E_p^{+1}-1\right)p\Pi(n,p,\tau), \end{aligned} \tag{2}$$

where $\Pi(n,p,\tau)$ is the probability that at time τ there are n genes in state G and p protein molecules according to the CME, and E_n^m and E_p^m are step operators such that when they act on a function $f \equiv f(n,p)$, their action is $E_n^m f(n,p) = f(n+m,p)$ and $E_p^m f(n,p) = f(n,p+m)$. The nondimensional reaction rates are given by

$$q_{\text{off}} = \frac{k_{\text{off}}}{c}, \quad q_{\text{on}} = \frac{k_{\text{on}}}{c}, \quad q_1 = \frac{k_1}{c}, \quad q_2 = \frac{k_2}{c}.$$

The CFPE for the reaction system Eq. (1) (with dimensionless time units, $\tau = ct$) is given by

$$\begin{aligned}\partial_\tau P(n,p,\tau) = {} & -\partial_n\left\{\left[q_{\text{off}}(N-n) - q_{\text{on}}n\right]P(n,p,\tau)\right\} \\ & - \partial_p\left\{\left[q_1 n + q_2(N-n) - p\right]P(n,p,\tau)\right\} \\ & + \tfrac{1}{2}\partial_n^2\left\{\left[q_{\text{off}}(N-n) + q_{\text{on}}n\right]P(n,p,\tau)\right\} \\ & + \tfrac{1}{2}\partial_p^2\left\{\left[q_1 n + q_2(N-n) + p\right]P(n,p,\tau)\right\}, \end{aligned} \tag{3}$$

where $P(n,p,\tau)$ is the probability that at time τ there are n genes in state G and p protein molecules according to the CFPE.

1. The quasistationary approximation

Next we solve the CME under the condition that the timescales governing the decay of small fluctuations about the steady-state mean number of molecules of G and P are well separated, i.e., the quasistationary approximation (QSA) of the CME. Since the system Eq. (1) consists of purely first-order reactions, the equations for the means $\langle n\rangle$ and $\langle p\rangle$ as obtained from the CME Eq. (2) are precisely given by the conventional rate equations: $\partial_\tau\langle n\rangle = -q_{\text{on}}\langle n\rangle + q_{\text{off}}(N-\langle n\rangle)$ and $\partial_\tau\langle p\rangle = q_1\langle n\rangle + q_2(N-\langle n\rangle) - \langle p\rangle$. The two characteristic nondimensional timescales are given by the absolute value of the inverse of the eigenvalues of the Jacobian of the above system of rate equations and are: $\tau_G = (q_{\text{on}} + q_{\text{off}})^{-1}$ and $\tau_P = 1$, where the former governs the decay of small fluctuations in G and the latter the same but for P. Clearly gene switching between the two states G and G^* is much slower than the rest of the processes in the system whenever $\tau_G \gg 1$, i.e., the protein reaches steady-state in a time much shorter than the time it takes for a gene to switch from one state to another.

Now we approximately solve the CME Eq. (2) in the quasistationary limit given by $\varepsilon = \tau_G^{-1} \ll 1$. Rescaling time by $\tau \to \varepsilon\tau$ we obtain the following master equation:

$$\partial_\tau \Pi(n,p,\tau) = \frac{1}{\varepsilon}\mathcal{L}^0\Pi(n,p,\tau) + \mathcal{L}^1\Pi(n,p,\tau), \tag{4}$$

where the two operators $\mathcal{L}^0$ and $\mathcal{L}^1$ are given by

$$\mathcal{L}^0 = [q_1 n + q_2(N-n)]\left(E_p^{-1}-1\right) + \left(E_p^{+1}-1\right)p, \tag{5}$$

$$\mathcal{L}^1 = \alpha\left(E_n^{+1}-1\right)n + \beta\left(E_n^{-1}-1\right)(N-n), \tag{6}$$

and $\alpha = q_{\text{on}}/(q_{\text{on}} + q_{\text{off}})$ and $\beta = 1-\alpha$. Note that $\mathcal{L}^0$ acts only on the protein numbers p while $\mathcal{L}^1$ acts only on the gene numbers n.

In order to solve Eq. (4) in the limit of small ε, we consider the perturbation ansatz:

$$\Pi(n,p) = \Pi_0(n,p) + \varepsilon\Pi_1(n,p) + \ldots + \varepsilon^i\Pi_i(n,p) + \ldots$$

Substituting the latter in Eq. (4) and comparing coefficients of powers of ε we obtain the following equations:

$$O\left(\frac{1}{\varepsilon}\right) : \mathcal{L}^0\Pi_0 = 0, \tag{7}$$

$$O(1) : \mathcal{L}^0\Pi_1 + \mathcal{L}^1\Pi_0 = \partial_\tau\Pi_0 = 0. \tag{8}$$

Note that $\partial_\tau\Pi_0 = 0$ by the assumption of steady-state. We can write $\Pi_0(n,p) = \Pi_0(p\,|n)\mu(n)$, where $\Pi_0(p|n)$ is the stationary density for P given the number of G molecules is n, and $\mu(n)$ is the marginal stationary distribution for G. Summing the $O(1)$ equation over p, we obtain

$$\sum_{p\in\mathbb{N}}[\mathcal{L}^0\Pi_1(n,p)] + \mathcal{L}^1\left[\sum_{p\in\mathbb{N}}\Pi_0(p\,|n)\mu(n)\right] = 0. \tag{9}$$

The first term on the left-hand side is zero by the definition of $\mathcal{L}^0$ in Eq. (5). The second term simplifies by the normalization condition $\sum_{p\in\mathbb{N}}\Pi_0(p\,|n) = 1$. Thus, Eq. (9) reduces to

$$\mathcal{L}^1\mu(n) = 0,$$

which possesses a unique normalized solution given by

$$\mu(n) = \frac{\binom{N}{n}}{(1+\lambda)^N}\lambda^n, \quad n \in \{0,\ldots,N\}, \tag{10}$$

where $\lambda = \beta/\alpha = (1-\alpha)/\alpha = q_{\text{off}}/q_{\text{on}}$. From the $O(\varepsilon^{-1})$ equation we obtain

$$\mu(n)\,\mathcal{L}^0\Pi_0(p\,|n) = 0.$$

This equation can be easily solved yielding the Poissonian:

$$\Pi_0(p\,|n) = \frac{1}{p!}\left[q_1 n + q_2(N-n)\right]^p e^{-[q_1 n + q_2(N-n)]}. \tag{11}$$

Finally, multiplying Eq. (10) and Eq. (11) and summing over n, we obtain by the law of total probability the stationary distribution of the protein numbers in the limit of small ε:

$$\Pi(p) \approx \sum_{n=0}^{N}\binom{N}{n}\frac{\lambda^n}{p!}\frac{\left[q_1 n + q_2(N-n)\right]^p}{(1+\lambda)^N}e^{-[q_1 n + q_2(N-n)]}. \tag{12}$$

In principle a similar quasistationary limit can be applied to the CFPE Eq. (3). In practice, however, the equation thus obtained cannot be reduced beyond an integral that has no closed form solution; thus, in what follows we obtain the stationary distribution of the protein numbers of the CFPE numerically (see later for details).

2. CME versus CFPE and CCLE solutions

Let Ω be the volume of the compartment in which the chemical reaction network Eq. (1) is confined. Furthermore, let $\phi_P = p/\Omega$ be the protein concentration and $\phi_N = N/\Omega$ be the (constant) total gene concentration. We now study the number of modes of the quasistationary distribution of ϕ_P as a function of Ω; in this thought experiment, the volume Ω is varied at constant ϕ_N such that an increase in volume, necessarily translates into a proportionate increase in the total number of genes (this also implies that the number of proteins increases with the volume). Now the CME distribution of ϕ_P is given by $\pi(\phi_P) = \Omega\Pi(\phi_P\Omega)$. This probability distribution solution consists of a superposition of $N+1$ Poisson distributions; this is since there are $N+1$ combinations of N molecules, which can be in one of two states. This implies that $\pi(\phi_P)$ is generally multimodal, with at most $N+1$ modes. Since N increases with Ω, we would expect the modality of $\pi(\phi_P)$ to increase with the volume, if the Poissonians are well separated. On the other hand, given that the deterministic rate equations of the chemical system are monostable, we also know, by the system-size expansion [1], that in the thermodynamic limit of large volumes, the probability distribution $\pi(\phi_P)$ tends to a Gaussian and thus unimodal. Hence, the overall picture is that the number of modes of $\pi(\phi_P)$ should increase with Ω for Ω less than some critical volume Ω^* and decrease with increasing volume for $\Omega > \Omega^*$. The smallest volume possible is that for which there is one gene $N = 1$; hence the maximum number of modes in the limit of small volumes is 2.

In Fig. 1, we plot the QSA solution $\pi(\phi_P)$ for four different volumes with parameters $\phi_N = 1$, $q_{\text{on}} = q_{\text{off}} = 10^{-3}$, $q_1 = 50$, $q_2 = 250$; we compare this with the solution from the CFPE and exact stochastic simulations of the CME using Gillespie's stochastic simulation algorithm (SSA) [15]. Note that for the chosen parameters, $\varepsilon = 2 \times 10^{-3} \ll 1$, which implies timescale separation; this is reflected in the excellent agreement between the analytical approximation (QSA) and the SSA. As predicted above, the modality of the probability distribution of the CME goes through a maximum as the volume is progressively increased, with the number of modes for very low and large volumes being 2 and 1, respectively. Thus, the CME predicts noise-induced multimodality as the volume is decreased beyond some critical value; we call this "noise-induced" since the particle numbers becomes smaller with the volume and the size of intrinsic noise correspondingly increases. The CFPE solution is obtained by discretizing the partial differential equation (PDE) Eq. (3) using the continuous Galerkin finite element method [16] over a triangulation of the domain $[0,N] \times [0,N^*]$ where $N^* > 0$ is some artificial maximum protein number, which is chosen sufficiently large such that its value makes no significant difference to the solution; no-flux boundary conditions are imposed along the domain boundaries. Note that the CFPE, unlike the CME, does not predict noise-induced multimodality as the volume is decreased from 100 to 1—rather it is unimodal for all four volumes in Fig. 1. Note also that for some volumes below $\Omega = 1$, the CFPE does predict two modes of the probability distribution (e.g., a mode at zero and one at a nonzero concentration for $\Omega = 1/2$); however, for such volumes the total number of genes is less than 1 (since $\phi_N = 1$); hence, we can more precisely state that over the whole range of physically meaningful volumes, the CFPE is unimodal. Note that the no-flux (reflective) boundary conditions on the CFPE are artificial in the sense that unlike the CME, the CFPE does not naturally lead to a restriction of gene numbers between 0 and N—the imposition of such artificial reflective conditions can lead to undesirable artefacts in the CFPE predictions (see, for example, Ref. [4]); to this end, we repeated our simulations using the recently developed complex chemical Langevin equation (CCLE) [4], which avoids the artificial boundary problems. More specifically, we considered the following complex-valued system of Itô stochastic differential equations (SDEs):

$$
\begin{aligned}
d\Phi(t) &= \{q_{\text{off}}[\phi_N - \Phi(t)] - q_{\text{on}}\Phi(t)\}\, dt + \sqrt{\frac{q_{\text{off}}}{\Omega}[\phi_N - \Phi(t)]}\, dB_1(t) + \sqrt{\frac{q_{\text{on}}}{\Omega}\Phi(t)}\, dB_2(t) \\
d\Psi(t) &= \{q_1\Phi(t) + q_2[\phi_N - \Phi(t)] - \Psi(t)\}\, dt + \sqrt{\frac{q_1}{\Omega}\Phi(t)}\, dB_3(t) + \sqrt{\frac{q_2}{\Omega}[\phi_N - \Phi(t)]}\, dB_4(t) + \sqrt{\frac{\Psi(t)}{\Omega}}\, dB_5(t),
\end{aligned}
\tag{13}
$$

where $B_k(t)$ are pairwise independent, standard real Brownian motions, for $k = 1, \ldots, 5$. This SDE arises as the complexification of the chemical Langevin equation (CLE) [17] corresponding to Eq. (3) obtained by extending the state space from $\mathbb{R}^2$ to $\mathbb{C}^2$. The states of the gene and protein processes are then recovered by taking

$$\phi_n(t) = \text{Re}\,\Phi(t) \quad \text{and} \quad \phi_P(t) = \text{Re}\,\Psi(t).$$

Although Eq. (13) appears identical in form to the original CLE, as the state space is complex, the breakdown that typically occurs with the CLE when the arguments of one of the square roots becoming negative is avoided, without having to impose any artificial boundary conditions. Moreover, as the scheme in Eq. (1) represents a first-order chemical system, it is straightforward to show that the mean and variance of the complex process $[\Phi(t), \Psi(t)]$ equal those of the original system. To generate samples of the stationary distribution of Eq. (13) we used an Euler-Maruyama discretization with time-step size $\Delta t = 10^{-2}$ to generate a single realization of $T = 10^8$ time-units long. Samples of the chain were

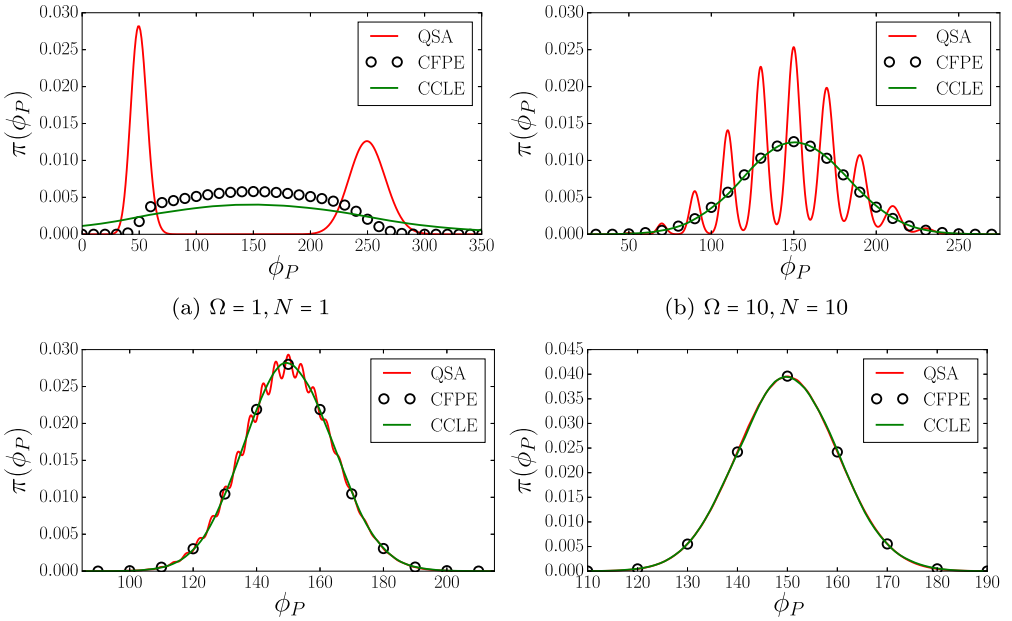

(a) $\Omega = 1, N = 1$ (b) $\Omega = 10, N = 10$

(c) $\Omega = 50, N = 50$ (d) $\Omega = 100, N = 100$

FIG. 1. (Color online) Comparison of the stationary distribution of protein concentration obtained from SSA simulations with the QSA solution $\pi(\phi_P)$ obtained by Eq. (12), the numerical solution of the CFPE given by Eq. (3) and the CCLE given by Eq. (13) for different values of volume. The volumes used are $\Omega = 1, 10, 50, 100$ for (a)–(d), respectively; since the gene concentration ϕ_N is fixed to 1, this implies that the gene copy numbers N are the same as the volumes. Parameters (see text) are such that timescale separation is enforced. The QSA and SSA predict multimodality below a certain volume whereas the CFPE predicts a unimodal distribution for all volumes.

obtained every 10^3 time-units, from which a histogram of $\phi_P(t) = \mathrm{Re}\,\Psi(t)$ was generated. We plot the resulting distribution in Fig. 1. For $\Omega \geqslant 10$ we see very good agreement between the CCLE and corresponding SSA simulations. The only significant difference arises in the low volume ($\Omega = 1$) case. In this case, the artificial imposition of reflecting boundary conditions significantly alters the distribution of the CFPE, causing it to concentrate around the mode at $\phi_P = 150$. On the other hand, in this regime, the CCLE spends significant time exploring the negative values of ϕ_P. The corresponding stationary distribution thus exhibits heavier tails, giving nonnegligible mass to negative values of ϕ_P, however remains unimodal with mode at $\phi_P = 150$.

The behavior elucidated in Fig. 1 is not particular to the parameter set used; in Fig. 2 we show the number of modes of the QSA distribution of protein $\pi(\phi_P)$ as a function of the volume Ω for eight different parameter sets (with fixed $\phi_N = 1$, $\lambda = 1$). In all cases, the number of modes is 1 for large volumes, increases as the volume decreases, and reaches a maximum at some critical volume; as the volume is decreased further, the number of modes steadily decreases until it reaches a value of 2 at the lowest volume of $\Omega = 1$ (below this volume the total number of genes is less than one and hence unrealistic). The CFPE probability distribution solution is unimodal for all volumes.

A comparison of Figs. 2(a) and 2(b) shows that the dimensionless parameter $\delta = \sqrt{q_2} - \sqrt{q_1}$ (and not the individual

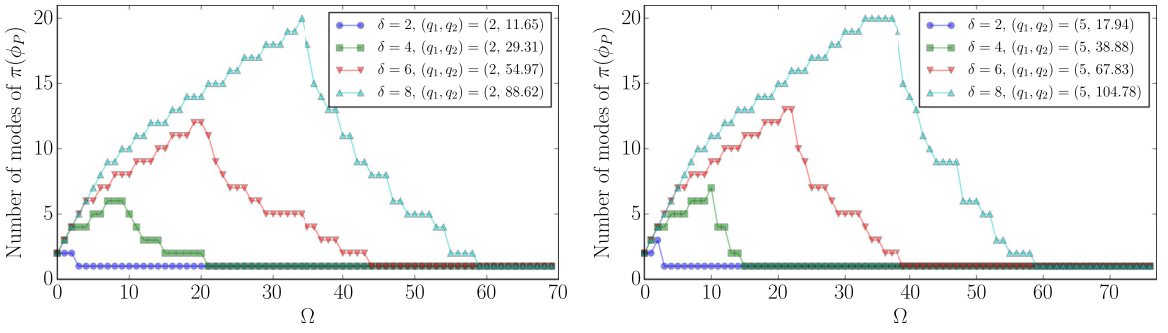

(a) $q_1 = 2$ (b) $q_1 = 5$

FIG. 2. (Color online) Plot of the number of modes of $\pi(\phi_P)$ as a function of the volume Ω, for different values of $\delta = \sqrt{q_2} - \sqrt{q_1}$. The larger is the difference between the production rates q_1, q_2, the larger is the volume range over which the stationary distribution of the CME is multimodal; in contrast, the solution of the CFPE is unimodal for all volumes.

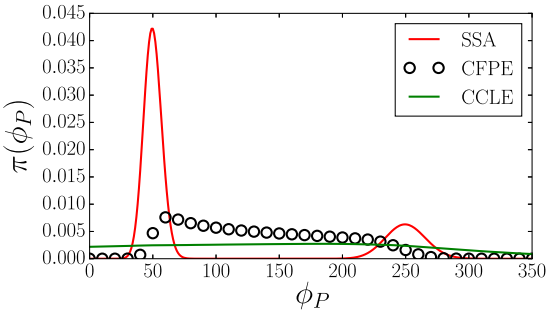

(a) $\Omega = 1, N = 1$

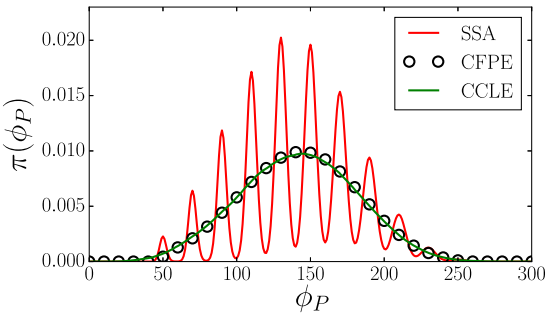

(b) $\Omega = 10, N = 10$

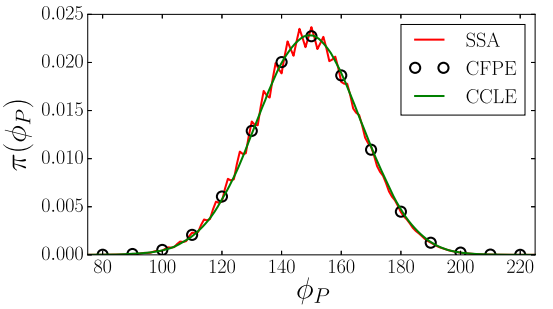

(c) $\Omega = 50, N = 50$

FIG. 3. (Color online) Comparison of the stationary distribution of protein concentration obtained from SSA simulations, the numerical solution of the CFPE for different values of volume, Ω, and simulations of the CCLE for the genetic feedback loop Eq. (14). See text for parameter values. Note that as for the gene feedback loop with no feedback (Fig. 1), the CFPE does not capture the onset of multimodality as the volume (and the number of gene molecules N) is decreased below a critical value.

values of q_1 and q_2) appears to be the principle factor determining the maximum number of modes of the probability distribution, as well as the critical volume at which this occurs. In particular, the larger δ is, the larger the volume is (and the associated number of genes), above which the probability distribution of the CME becomes unimodal and agrees with the CFPE. A heuristic explanation of this is as follows. For the case of one gene ($N = 1$), the QSA solution Eq. (12) predicts two modes, a Poissonian with mean and variance equal to q_1 and a second Poissonian with mean and variance equal to q_2. Now say that $q_1 < q_2$; then the condition of well-separated Poissonians can be formulated as $q_1 + \sqrt{q_1} \ll q_2 - \sqrt{q_2}$, which is equivalent to $\delta = \sqrt{q_2} - \sqrt{q_1} \gg 1$. The larger δ is, the more pronounced the bimodal character of the distribution at $N = 1$; hence, one would expect a larger total number of genes is needed for the multimodality to be washed away—this is consistent with the role played by δ in Fig. 2.

B. Gene regulatory system with feedback

We now consider a variation of scheme Eq. (1) whereby the switching between the two gene states is mediated by protein binding:

$$G + P \underset{k'_{\text{off}}}{\overset{k'_{\text{on}}}{\rightleftharpoons}} G^*, \quad G \xrightarrow{k'_1} G + P, \quad G^* \xrightarrow{k'_2} G^* + P, \quad P \xrightarrow{c'} \emptyset. \tag{14}$$

This system constitutes a genetic negative feedback loop if $k'_2 < k'_1$ and a positive feedback loop if $k'_2 > k'_1$. An exact solution of the CME for the case of one gene has been reported in Ref. [18]. We study this example numerically using the CME, the CFPE, and the CCLE for a positive feedback system with N genes and the parameter set: $c' = 1, k'_{\text{on}} = 6.67 \times 10^{-6}, k'_{\text{off}} = 0.001, k'_1 = 50, k'_2 = 250, \phi_N = 1$ for three different volumes $\Omega = 1, 10, 50$. Note that as before the number of genes equals $N = \phi_N \Omega$ and hence the three volumes chosen correspond to a system with 1, 10, and 50 gene copy numbers, respectively. Note that the parameters are chosen so that timescale separation conditions are met. The step-size, sampling rate, and simulation length used for the simulation of the CCLE are the same as the previous example. The results of simulations using the SSA, the Galerkin finite element method for the CFPE, and simulations of the CCLE are shown and contrasted in Fig. 3. As for the scheme Eq. (1) studied in the previous section, the CFPE does not reproduce the noise-induced multimodality predicted by the CME. Once again, the only significant difference between the CFPE and CCLE arises in the low-volume scenarios ($\Omega = 1$), due to the fact that the CCLE spends a significant amount of time exploring negative values of ϕ_P; however, the resulting distribution remains unimodal.

III. CONCLUSION

We have shown in this paper, by means of two exemplary gene circuits, that the CFPE does not always capture the noise-induced multimodality predicted by the CME. This implies that there are two different types of systems: those for which the CFPE can capture the inherent noise-induced multimodality, such as the foraging ant model studied in Ref. [12], and those for which the CFPE fails to predict the phenomenon. The main difference between these two classes of systems is that in the former the switching between different states is described by the CFPE's diffusion term (see discussion in Ref. [12]), whereas the multimodality studied in this article cannot be so described.

We note that the probability distribution of the CME Eq. (12) is a superposition of Poissonians, each one associated with an element of the set $\{(0,N),(1,N-1),\ldots,(N,0)\}$, which describes the possible combinations of genes in states G and G^*—it is this direct association between the distribution and the inherent discreteness of the system that leads to the CFPE's inability to capture the multimodality of the CME.

Hence, in some sense the phenomenon described in this paper may be more aptly described as discreteness-induced multimodality.

Thus, we generally expect the CFPE to fail to reproduce noise-induced multimodality whenever the multimodality can be explicitly related to the switching of a molecule between a discrete number of conformational states; this is since the CFPE is a continuum approximation and hence cannot capture discreteness. This is the case of a broad class of gene regulatory networks under timescale separation conditions [11]. Since enzymes also switch between a number of discrete conformational states [19] we also expect the CFPE to fail to reproduce multimodality in the enzyme product distributions under certain conditions.

ACKNOWLEDGMENTS

The research leading to these results has received funding from the European Research Council under the European Community's Seventh Framework Programme (FP7/2007-2013)/ERC Grant Agreement No. 239870 (A.D., S.L., R.E.). T.V. acknowledges the support of RVO (Grant No. 67985840) and from the People Programme (Marie Curie Actions) of the European Union's Seventh Framework Programme (FP7/2007–2013) under REA Grant Agreement No. 328008. R.E. would also like to thank the Royal Society for a University Research Fellowship; Brasenose College, University of Oxford, for a Nicholas Kurti Junior Fellowship; and the Leverhulme Trust for a Philip Leverhulme Prize. These prize funds also supported a research visit of R.G. in Oxford.

[1] N. G. van Kampen, *Stochastic Processes in Physics and Chemistry* (Elsevier, Amsterdam, 2007).
[2] W. Horsthemke and L. Brenig, Z. Physik B **27**, 341 (1977).
[3] R. Grima, P. Thomas, and A. V. Straube, J. Chem. Phys. **135**, 084103 (2011).
[4] D. Schnoerr, G. Sanguinetti, and R. Grima, J. Chem. Phys. **141**, 024103 (2014).
[5] R. Erban, S. J. Chapman, I. G. Kevrekidis, and T. Vejchodský, SIAM J. Appl. Math. **70**, 984 (2009).
[6] P. Thomas, A. V. Straube, J. Timmer, C. Fleck, and R. Grima, J. Theor. Biol. **335**, 222 (2013).
[7] P. Hanggi, H. Grabert, P. Talkner, and H. Thomas, Phys. Rev. A **29**, 371 (1984).
[8] W. Horsthemke and R. Lefever, *Noise-Induced Transitions: Theory and Applications in Physics, Chemistry, and Biology* (Springer, Berlin, 1984).
[9] T. Kepler and T. Elston, Biophys. J. **81**, 3116 (2001).
[10] H. Qian, P-Z. Shi and J. Xing, Phys. Chem. Chem. Phys. **11**, 4861 (2009).
[11] P. Thomas, N. Popovic, and R. Grima, Proc. Natl. Acad. Sci. U.S.A. **111**, 6994 (2014).
[12] T. Biancalani, L. Dyson, and A. J. McKane, Phys. Rev. Letts. **112**, 038101 (2014).
[13] V. Shahrezaei and P. S. Swain, Proc. Natl. Acad. Sci. U.S.A. **105**, 17256 (2008).
[14] B. Alberts *et al.*, *Molecular Biology of the Cell* (Garland Publishing, New York, 1994).
[15] D. T. Gillespie, J. Phys. Chem. **81**, 2340 (1977).
[16] S. Larsson and T. Vidar, *Partial Differential Equations with Numerical Methods* (Springer, Berlin, 2008).
[17] D. T. Gillespie, J. Chem. Phys. **113**, 297 (2000).
[18] R. Grima, D. Schmidt, and T. J. Newman, J. Chem. Phys. **137**, 035104 (2012).
[19] B. P. English, W. Min, A. M. van Oijen, K. T. Lee, G. Luo, H. Sun, B. J. Cherayil, S. C. Kou, and X. S. Xie, Nat. Chem. Biol. **2**, 87 (2006).